energies

MDPI

Article

Analysis of Coupled Liquid Air Energy Storage and Liquefied Natural Gas Cold Energy Cascade Utilization System

Zetong Li [1], Xiaolei Si [2], Yongchao Zhao [3], Hongyan Zhao [2], Zheng Cai [2] and Yingjun Guo [1,*]

[1] School of Electrical Engineering, Hebei University of Science and Technology, Shijiazhuang 050027, China; 2023102123@stu.hebust.edu.cn
[2] Caofeidian Xintian LNG Co., Ltd., Tangshan 063200, China; sixiaolei@suntien.com (X.S.); zhaohongyan@suntien.com (H.Z.); caizheng@suntien.com (Z.C.)
[3] Suntien Green Energy Co., Ltd., Shijiazhuang 050011, China; zhaoyongchao@suntien.com
* Correspondence: guoyj@hebust.edu.cn

Abstract: The vaporization of liquefied natural gas (LNG) liberates a substantial quantity of cold energy. If left unutilized, this cold energy would cause significant energy waste. Currently, both domestic and international cold energy utilization strategies are rather simplistic and unable to fully capitalize on the wide temperature range feature inherent in LNG cold energy. This study presents a three-tiered cold energy utilization system that integrates liquid air energy storage (LAES), cold energy power generation, and cold energy air conditioning. Moreover, during the LNG vaporization process, the thermal discharge from the power plant is utilized as a heat source to boost energy utilization efficiency and environmental performance. This research develops thermodynamic and economic evaluation models for the coupled system. It uses Aspen HYSYS V14 software to conduct process simulation, analyze cycle efficiency and exergy efficiency, and assesses the system's economic feasibility by applying the net present value (NPV) method, which is based on the regional electricity prices of an LNG receiving station in Tangshan. The results show that the system attains a cycle efficiency of 105.83% and an exergy efficiency of 55.89%, representing a 6.18% improvement over traditional LAES systems. The system yields an annual revenue of CNY 77.06 million, with a net present value (NPV) of CNY 566.41 million and a capital payback period of merely 2.53 years, demonstrating excellent economic feasibility. This study offers crucial references and a foundation for the engineering application of LNG cold energy in energy storage and power plant peak regulation.

Keywords: liquefied natural gas; liquid air energy storage; cold energy; cascade utilization; cold energy power generation

check for updates

Academic Editor: Adrian Ilinca

Received: 13 February 2025
Revised: 7 March 2025
Accepted: 11 March 2025
Published: 13 March 2025

Citation: Li, Z.; Si, X.; Zhao, Y.; Zhao, H.; Cai, Z.; Guo, Y. Analysis of Coupled Liquid Air Energy Storage and Liquefied Natural Gas Cold Energy Cascade Utilization System. *Energies* **2025**, *18*, 1415. https://doi.org/10.3390/en18061415

Copyright: © 2025 by the authors. Licensee MDPI, Basel, Switzerland. This article is an open access article distributed under the terms and conditions of the Creative Commons Attribution (CC BY) license (https://creativecommons.org/licenses/by/4.0/).

1. Introduction

Amidst the global energy transition toward low-carbon and clean energy systems, liquefied natural gas (LNG) plays a critical role as a transitional energy source, with its consumption continuing to rise steadily. However, due to technological limitations and cost barriers, substantial low-temperature cold energy generated during LNG regasification remains significantly underutilized. Studies report that approximately 830 MJ of cold energy is released per ton of LNG during regasification. Direct discharge of this cold energy into the environment not only results in substantial energy loss but also exacerbates thermal pollution [1–3]. Current applications of LNG cold energy include power generation, air separation, seawater desalination, and low-temperature CO_2 capture systems. Integration of LNG cold energy into these systems demonstrates significant improvements in energy

efficiency and exergy recovery rates [4,5]. In practice, the utilization efficiency of liquefied natural gas (LNG) cold energy remains suboptimal. In traditional LNG cold energy power generation technologies, the secondary medium approach, despite being more efficient than the direct expansion method, still fails to fully harness the cold energy of LNG. This inefficiency stems from the imperfect alignment between the condensation temperature of the intermediate medium and the vaporization curve of LNG. In current applications, the actual efficiency generally does not surpass 30%, leading to substantial cold energy waste. Currently, air separation using LNG cold energy is the predominant method for harnessing LNG cold energy, accounting for more than 40% of applications. Nevertheless, the utilization efficiency of LNG cold energy in air separation units is relatively low, typically fluctuating within the range of 10% to 25%. Ref. [5] put forward an integrated system that consists of air separation, power generation, refrigeration, and ice thermal storage. The system, optimized by using the second-generation non-dominated sorting genetic algorithm (NSGA-II), achieved an exergy efficiency of 43% and a thermal efficiency of 48% when the LNG capacity was 70 t/h. Ref. [6] compares several relatively mature technologies for utilizing the cold energy of liquefied natural gas (LNG) and concludes that cold energy power generation is the most promising single method for widespread application. To make full use of LNG cold energy, Ref. [7] developed and optimized a dual-Rankine cycle power generation system which integrates the heat exchange between LNG cold energy utilization and propane–ethylene working fluids, thus providing valuable insights for enhancing power generation efficiency with LNG cold energy. In [8], an innovative incremental analysis method was used to thoroughly examine six LNG cold energy power generation systems, including the newly proposed parallel and cascaded combined cycles. A novel method was applied to set the system's minimum pressure above the atmospheric level to achieve optimal performance.

Liquid air energy storage (LAES), a novel large-scale physical energy storage technology, has attracted considerable attention in recent years because of its high energy density (approximately 700 MJ/m^3), flexible siting, and long service life [9–12]. The fundamental principle of LAES is to utilize electrical energy to liquefy air and store the liquefied air. During periods of peak electricity demand, the liquid air is vaporized under pressure to drive a turbine for power generation, thereby enabling the temporal and spatial transfer of electrical energy and contributing to grid peak shaving [13,14]. Nevertheless, traditional LAES systems face two significant bottlenecks. Firstly, the air liquefaction process requires a large amount of electrical energy for compression and refrigeration, which constitutes 60% to 70% of the total energy consumption during the energy storage phase and results in a relatively low system cycle efficiency (typically ranging from 50% to 70%). Secondly, in the energy release phase, the thermal energy required for the vaporization of liquid air has to depend on external heat sources or heat storage media, which further elevates the system's complexity and cost.

Coupling the cold energy of liquefied natural gas (LNG) with liquid air energy storage (LAES) technology presents an innovative solution to the aforementioned problems. During the vaporization of LNG, the low-temperature cold energy released can substitute for the electrically driven refrigeration process in traditional LAES systems and be directly utilized for air liquefaction. This substantially decreases the electrical energy consumption during the energy storage phase. In recent years, researchers have endeavored to incorporate LNG cold energy into LAES systems. Ref. [15] combines the liquid air energy storage process with LNG regasification and proposes a novel cryogenic liquid air energy storage system. Ref. [16] proposes an integrated liquid air energy storage system with parallel power generation. This system demonstrates optimal performance in power generation and economic benefits. Under basic operating conditions, the daily net output power of

LAES can reach 94.8 kJ/kg of LNG. Ref. [17] presents an integrated system for utilizing LNG cold energy and waste heat recovery (WHR) in the cement industry, which is based on LAES (LNG-LAES-WHR). The system is optimized by adopting a four-stage compression and expansion process, with R601 as the working fluid. Ref. [18] proposes an innovative power management system design. This design combines a series of Brayton cycles and two reheated Rankine cycles with the LAES system and incorporates liquid hydrogen regasification processes. This configuration offers enhanced flexibility to respond to power demand and achieves higher energy efficiency and capacity. Ref. [19] investigates an advanced integrated energy system. This system couples biomass and LNG complementary energy supply with LAES. The system mainly consists of two-stage organic Rankine cycles, LAES, and combined gas–steam cycles. The thermodynamic parameters of the system are optimized by using an adaptive genetic algorithm. The economic and exergy performance of the system is analyzed, considering factors such as the mixed combustion ratio, turbine pressure parameters, compressed air utilization rate, and fuel prices. Nevertheless, the majority of studies have not fully tapped into the potential of "temperature matching and cascaded recovery" of liquefied natural gas (LNG) cold energy. The broad temperature spectrum of LNG cold energy, spanning from −162 °C to the ambient temperature, can successively satisfy multi-level demands [20–25]. Nevertheless, existing system designs frequently concentrate on a single temperature range, giving rise to substantial exergy losses and inadequate overall utilization efficiency.

Based on this, this study proposes a liquid air energy storage system for the tertiary collaborative utilization of LNG cold energy. It innovatively integrates LAES, cold energy power generation, and cold energy air conditioning. During the energy storage phase, surplus electricity during off-peak periods drives compressors, while the cascaded cold energy of LNG and liquid propane is introduced to achieve efficient air liquefaction. During the energy release phase, the vaporization of liquid air drives turbines for power generation. Subsequently, the mid-grade cold energy of LNG is recovered for power generation via an organic Rankine cycle (ORC), and the low-grade cold energy is utilized for cooling the office area in front of the vaporization station. A thermodynamic model is constructed using Aspen HYSYS V14 to quantify the enhancement of system exergy efficiency through cascaded cold energy utilization. Combined with the peak and valley electricity pricing policy of a certain LNG receiving station in Tangshan, the net present value method is employed to assess the system's economic viability. This research aims to break through the technological barriers of traditional LAES and LNG cold energy utilization, providing important references and a basis for the engineering application of LNG cold energy in energy storage and power plant peak regulation.

2. System Process Flow

The LNG cold energy cascade utilization system comprises a liquid air energy storage system (LAES), a liquid air energy release system, a cold energy power generation system, and a cold energy air conditioning system. The system structure is illustrated in Figure 1, with LNG serving as the cold source and the power plant's warm wastewater, which contains residual heat, acting as the heat source. Prior to air storage, the air must be pretreated to remove moisture, carbon dioxide, and hydrocarbons to prevent freezing during the liquefaction process. The purified air serves as the feedstock for the liquefaction process [26]. The system operates in two modes: energy storage and energy release.

The energy storage mode operates during off-peak electricity periods. First, atmospheric-pressure LNG is pressurized to 7500 kPa by pump P1. During the energy storage process, valve Z1 is open while Z2 is closed. Surplus electricity from the grid drives a three-stage air compressor, which pressurizes and cools ambient air through three stages

of compression and inter-stage cooling. LNG and liquid propane from the cold storage device sequentially pass through four heat exchangers (HX4, HX3, HX2, HX1) to recover the compression heat generated by the air compressor. The warmed propane is stored in the propane thermal storage tank (PTST). The liquefied compressed air enters the cryogenic box for further cooling before being throttled through a J-T valve, facilitating liquefaction. The resulting liquid air is stored at atmospheric pressure and −192 °C. Any unliquefied cold air is returned to the cryogenic box to assist with cold storage. The low-temperature natural gas exiting heat exchanger HX1 enters the (ORC) of the cold energy power generation system. It exchanges heat with an intermediate medium, propane, in heat exchanger HX-ORC1. The liquefied propane is pressurized by pump P2 and vaporized by exchanging heat with the thermal discharge from the power plant in heat exchanger HX-ORC2. It then expands through turbine generator Tur5 to generate electricity, with the propane's temperature and pressure restored before returning to heat exchanger HX-ORC1 to complete the cycle. The natural gas, now warmed by the power generation section, enters the cold energy air conditioning part, where it exchanges heat with the air conditioning loop water in the air conditioning heat exchanger (HX-AIR) to provide cooling. Finally, the low-temperature natural gas is heated to 1 °C via heat exchange with the thermal discharge from the power plant in heat exchanger HX9, after which it is transported externally.

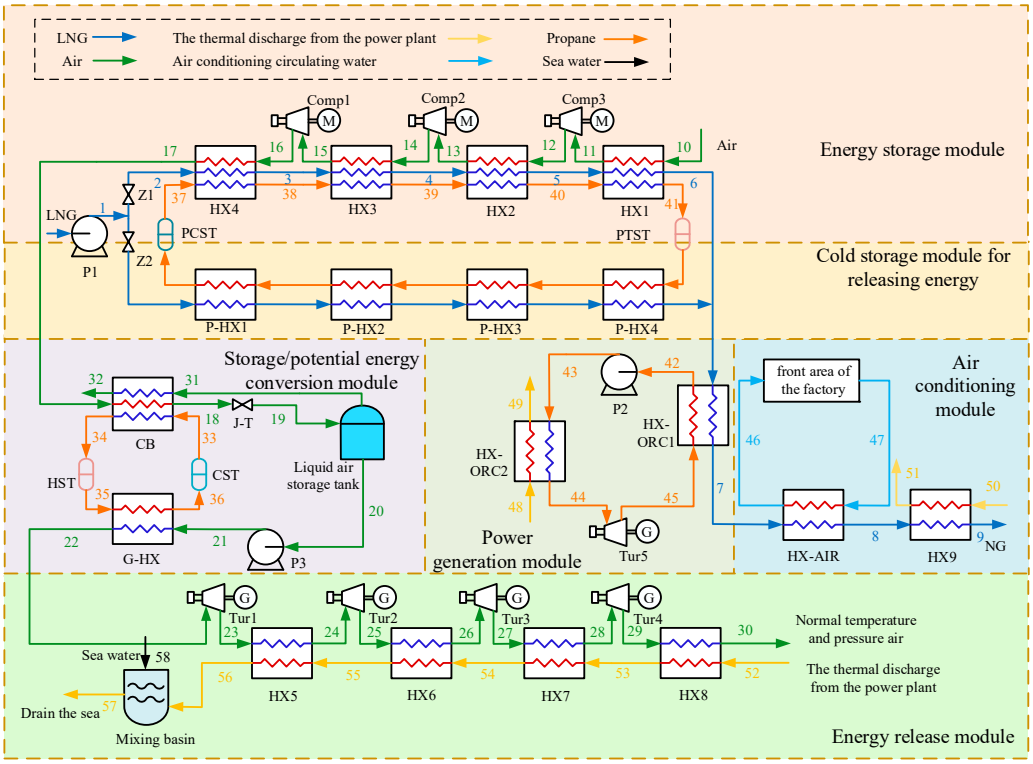


Figure 1. Schematic diagram of system structure.

The energy release mode operates during peak electricity periods. Valve Z2 is open while Z1 is closed. LNG is pressurized to 7500 kPa by pump P1 and then vaporized through the propane heat exchanger group (P-HX1 to P-HX4) in the cold storage device before entering the cold energy power generation section directly. The propane in the cold storage device is liquefied and stored in the propane cryogenic storage tank (PCST). Subsequently, the low-temperature natural gas is further warmed by the cold energy air conditioning system and finally heated to 1 °C by exchanging heat with the thermal discharge from the power plant in heat exchanger HX9 before being transported externally.

Simultaneously, liquid air exits the storage tank and is pressurized using low-temperature pump P3. The high-pressure liquid air is heated to near-ambient temperature via the vaporization heat exchanger G-HX. The high-pressure air then enters a four-stage expander, performing work to drive a generator and generate electricity, ultimately achieving peak shaving and valley filling.

During energy release and power generation, the liquid air storage tank activates its self-pressurizing device to maintain a stable internal pressure. To enhance energy efficiency, the gaseous cold air released from the storage tank during energy storage is recovered in the cryogenic box to aid cold storage. Selecting an efficient working fluid for intermediate energy storage depends on its isobaric heat capacity and operating temperature range. Propane is chosen for its high isobaric heat capacity and appropriate temperature range, with a melting point below −183 °C.

3. Parameter Setting and Model Analysis

3.1. Parameter Setting

This study utilizes Aspen HYSYS for modeling and calculations, applying the Peng–Robinson equation of state for property analysis. The LNG composition is presented in Table 1.

Table 1. LNG composition.

Molar Composition	Units	Components
N_2	% (mol)	0.23
CH_4	% (mol)	99.62
C_2H_6	% (mol)	0.13
C_3H_8	% (mol)	0
C_4H_{10} (n-Butane)	% (mol)	0.01
C_4H_{10} (Isobutane)	% (mol)	0.01
C_5H_{12} (n-Pentane)	% (mol)	0
total	% (mol)	100

It is assumed that the system is in a steady state during both energy storage and release modes, and pipeline pressure drop as well as temperature loss are not considered. The basic parameters of the entire system are shown in Table 2.

Table 2. Basic parameters of each component of the system.

Parametric	Numerical Value
LNG mass flow rate	207 t/h
LNG inlet pressure	101.3 kPa
LNG inlet temperature	−162 °C
NG outlet temperature	1 °C
NG outlet pressure	7500 kPa
Air mass flow rate	2.87×10^5 kg/h
Air compressor unit outlet pressure	3500 kPa
Liquid air pump outlet pressure	12,000 kPa
Four-stage air expansion unit outlet pressure	101.3 kPa
Propane mass flow rate	5.298×10^5 kg/h
The thermal discharge from the power plant temperature	35 °C
Mass flow rate of circulating medium in ORC system	1.25×10^5 kg/h
ORC system circulating pump load	66.98 kW
Turbine power generation efficiency	0.85
Air-conditioned water temperature range	7~12 °C

3.2. Model Analysis

3.2.1. Model Analysis of Cycle Efficiency

When the vaporization pressure is constant, the cold energy released by 1 kg of LNG when heated from −162 °C to temperature t can be calculated using the following formula:

$$E = H_t - H_{-162} \tag{1}$$

where E is the cold energy released by LNG (in kJ); H_t is the specific enthalpy of LNG at temperature t (in kJ). H_{-162} is the specific enthalpy of LNG at −162 °C (in kJ).

In this system study, the cycle efficiency is defined as the ratio of the net output electrical power generated by the released air to the net input electrical power consumed by the liquefaction of air. The output or input power of the expander, compressor, and pump can be calculated using the following formulas:

$$W_{Tur} = m_{AIR} \times (H_{in} - H_{out}) \tag{2}$$

$$W_{Comp} = m_{AIR} \times (H_{out} - H_{in}) \tag{3}$$

$$W_{Pump} = m_{AIR,ORC} \times (H_{out} - H_{in}) \tag{4}$$

During the liquid air energy storage phase, the total input electric power of the system is calculated as follows:

$$W_I = \sum_{i=1}^{3} W_{Compi} \tag{5}$$

During the liquid air energy release stage, the total output electric power of the system is calculated as follows:

$$W_O = \sum_{i=1}^{5} W_{Turi} - \sum_{i=1}^{3} W_{Pumpi} \tag{6}$$

The system circulation efficiency is calculated as follows:

$$\eta_{RT} = \frac{W_O}{W_I} \tag{7}$$

3.2.2. Exergy Efficiency Model Analysis

Exergy efficiency analysis is a thermodynamic assessment method rooted in the second law of thermodynamics, which evaluates the performance and quality of energy conversion and utilization processes.

The formula for calculating the exergy value of each logistics unit in the system is as follows:

$$E_i = m_i \times (H - H_0) - T_0(S - S_0) \tag{8}$$

The exergy balance equation is formulated as follows:

$$E_{xnetin} = \sum E_{xin} + \sum W_{in} \tag{9}$$

$$E_{xnetout} = \sum E_{xout} + \sum W_{out} \tag{10}$$

$$E_{xnetin} - E_{xnetout} = \sum L \tag{11}$$

$$E_{F,i} = E_{P,i} + E_{D,i} \tag{12}$$

Here, L denotes the exergy destruction rate (also referred to as the loss rate). The subscript "*net*" specifies the net exergy transfer rate. Net exergy is calculated as the

difference between total exergy input and work output, whereas the exergy destruction rate is calculated through exergy balance equations.

The formulae for calculating the efficiency of each piece of equipment in the system are as follows:

$$\eta_{\text{exi}} = \frac{E_{P,i}}{E_{F,i}} = 1 - \frac{E_{\text{D},i}}{E_{F,i}} \tag{13}$$

The system exergy efficiency is calculated as follows:

$$\eta_{\text{ex-overall}} = \frac{\sum_{i=1}^{5} W_{\text{Turi}} - \sum_{i=1}^{3} W_{\text{Pumpi}} + P_{\text{AIR}}}{E_{\text{LNG}} - E_{\text{NG}} + \sum_{i=1}^{3} W_{\text{Compi}}} \tag{14}$$

3.2.3. Economic Model Analysis

The net present value (NPV) method was used to assess the economic viability of the system process. The annual return is calculated as the product of the peak electricity price, the power generated during the energy release phase, and the number of operational hours, as follows:

$$\text{REV} = \left[\left(\sum_{i=1}^{5} W_{Turi} - \sum_{i=2}^{3} W_{Pumpi} \right) \times C_{ele,on} \times t_{on} \right] \times 365 \tag{15}$$

where $C_{ele,on}$ refers to the peak tariff, and t_{on} refers to the duration of energy release.

The annual operating cost (C_o) consists of maintenance and power consumption costs. The annual maintenance cost is set at 3% of the total capital cost, while the power consumption cost is calculated as the product of the trough-period tariff, the power consumed during the energy storage phase, and the number of operational hours [27]. The formula is as follows:

$$C_o = (W_I \times C_{ele,off} \times t_{off}) \times 365 + 0.03 \times C_c \tag{16}$$

where $C_{ele,off}$ refers to the valley tariff, t_{off} refers to the duration of energy storage, and refers to the total investment.

The net present value (NPV) is calculated as follows:

$$\text{NPV} = -C_c + \sum_{y=1}^{25} \frac{\text{REV} - C_o}{(1+r)^y} \tag{17}$$

The capital payback period *SPB* (in years) is calculated as follows:

$$SPB = \frac{C_C}{REV - C_O} \tag{18}$$

4. Results and Analysis

In this system, LNG sequentially undergoes heat exchange with air, the cold energy power generation ORC system, and the air conditioning loop water. After simulation using Aspen HYSYS V14, the key parameters of LNG (points 1–9) and air (points 10–30) in the system are shown in Tables 3 and 4, respectively. The heat exchange curves of LNG are shown in Figures 2 and 3. The total cold energy released by LNG when vaporized to 1 °C reaches 61,069.49 kW.

In the entire vaporization process of LNG, the cold energy released in the low temperature range (−162 °C to −80 °C) is the highest, reaching 18,802.5 kW, which accounts for approximately 44.37% of the total cold energy. As shown in Figure 2, this portion of the cold energy is absorbed by the LAES system, with liquid propane (points 37–41) and LNG (points 2–6) jointly providing cold energy for air liquefaction. As air flows through

HX1, LNG provides 4600 kW of cold energy and liquefied propane contributes 4562.16 kW, cooling the air to approximately −90 °C. Moving to HX2, LNG supplies 3737.5 kW and liquefied propane 4415 kW, reducing the air temperature to around −100 °C. In HX3, LNG provides 5002.5 kW and liquefied propane 2796.16 kW, cooling the air to approximately −110 °C. Finally, in HX4, LNG supplies 5462.5 kW and liquefied propane 9418.67 kW, lowering the air temperature to below −140 °C. Overall, the air absorbs 42,377.5 kW of cold energy from LNG and liquefied propane throughout the process.

Table 3. Key parameters for each state point of LNG.

Serial Number	Mass Flow/(kg/h)	Temperature/°C	Strains/kPa
1	207,000	−162.2	101.3
2	207,000	−158.9	7500
3	207,000	−131.8	7499
4	207,000	−109.2	7498
5	207,000	−94.71	7497
6	207,000	−80.43	7496
7	207,000	−45	7495
8	207,000	−22.27	7494
9	207,000	1	7493

Table 4. Key parameters for each state point of air.

Serial Number	Mass Flow/(kg/h)	Temperature/°C	Strains/kPa
10	287,270	24.85	100
11	287,270	−90.15	99
12	287,270	0.05	330
13	287,270	−100	329
14	287,270	−14.65	1090
15	287,270	−110	1089
16	287,270	−30.95	3500
17	287,270	−142.6	3499
18	287,270	−178.6	3498
19	287,270	−194.2	101
20	287,270	−194.4	101
21	287,270	−189.3	1200
22	287,270	14.85	1188
23	287,270	−61.99	3600
24	287,270	14.85	3560
25	287,270	−58.96	1080
26	287,270	14.85	1060
27	287,270	−57.48	320
28	287,270	14.85	320
29	287,270	−54.63	101
30	287,270	14	100

As depicted in Figure 3, the ORC system harnesses 14375 kW of cold energy from the medium temperature range (−80 °C to −45 °C) of LNG, constituting 33.92% of the total cold energy. Within the ORC system, propane, once liquefied by LNG cooling, undergoes a temperature cycle via heat exchange with the thermal discharge from the power plant, leading to minimal temperature variation in the ORC system (points 42–45). The high temperature range (−45 °C to 1 °C) of LNG contains 9200 kW of cold energy, with the cold energy air conditioning system absorbing 5002.5 kW, approximately 11.8% of the total cold energy. Concurrently, the air conditioning circulating water is cooled from 12 °C to 7 °C. The remaining 4197.5 kW of cold energy is absorbed by the thermal discharge

from the power plant, approximately 9.9% of the total cold energy. The natural gas is then transmitted to the pipeline upon meeting the external transmission requirements. Cascaded utilization of LNG cold energy enhances the energy utilization rate.

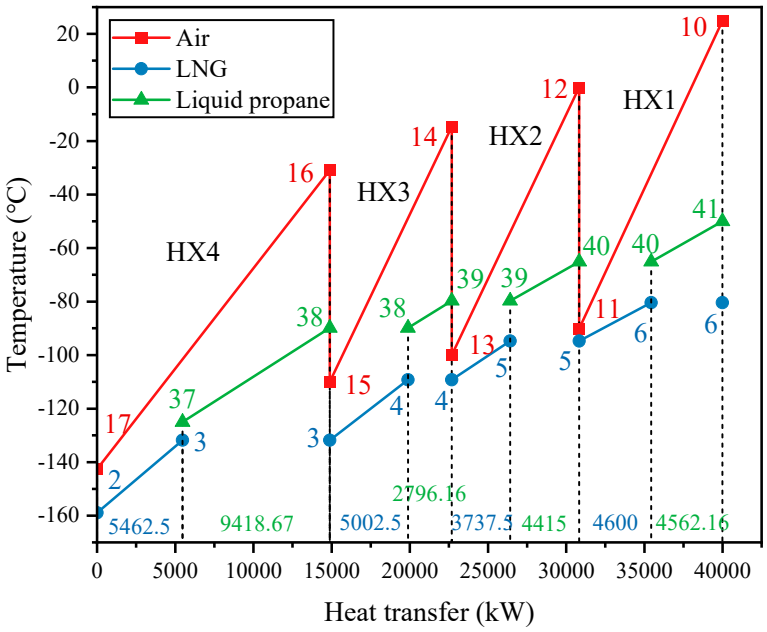


Figure 2. Cold and hot flow heat transfer curves of air energy storage section.

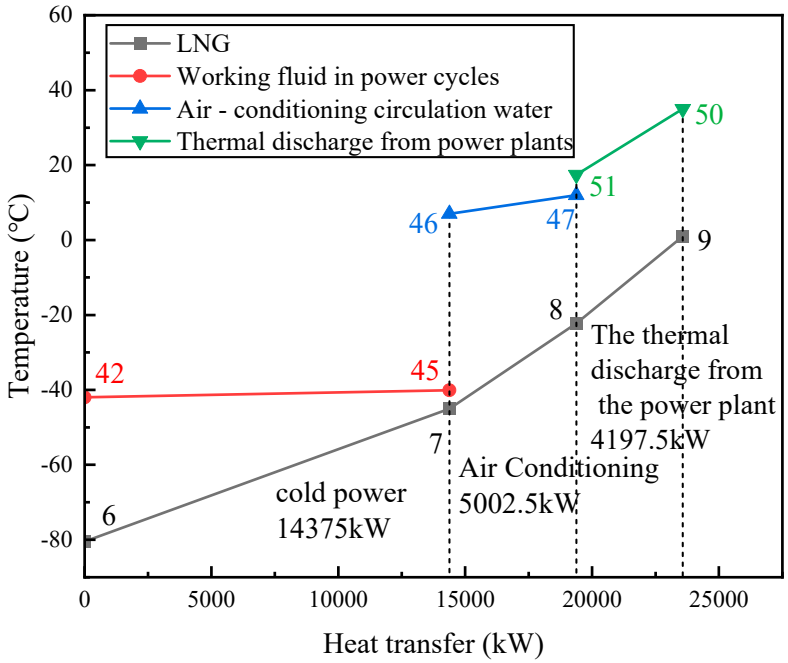


Figure 3. ORC, air conditioning system cold and heat flow heat transfer curve.

4.1. Cycle Efficiency Analysis

In conventional large-scale energy storage systems, cycling efficiency typically falls below 75%. However, when external energy is added to the system, cycling efficiency can exceed 100%. This increase in cycling efficiency directly boosts the net power output of the energy storage system, enhancing the economic returns of the project. After simulation, the system's performance parameters for the pump, compressor, and expander are shown in Table 5.

Table 5. Performance parameters of pump compressor and expander.

Equipment	Electrical Power/kW
P1	1178
P2	46.99
P3	1077
Comp1	7116
Comp2	6628
Comp3	5812
Tur1	4439
Tur2	4647
Tur3	4761
Tur4	4643
Tur5	2820

During the energy storage process, the power consumption of pumps P1, P2, and compressors Comp1, Comp2, and Comp3 totaled 20,780.99 kW, while the power generation of expander Tur5 amounted to 2820 kW, resulting in a net power consumption of 17,960.99 kW. In the energy release process, the power consumption of pumps P1, P2, and P3 totaled 2301.99 kW, while the combined power generation of expander units (Tur1, Tur2, Tur3, Tur4, and Tur5) reached 21,310 kW, resulting in a net power output of 19,008.01 kW. The cyclic efficiency of the new air–liquid energy storage system was 105.83%. Compared to conventional energy storage systems, this system not only receives surplus power from the grid but also utilizes LNG cooling for energy storage, resulting in a cycle efficiency greater than 100%.

4.2. Exergy Efficiency Analysis

4.2.1. Exergy Flow Analysis

Figure 4 illustrates the exergy flow diagram of the LNG cold energy utilization process. During the energy storage process, LNG at −162 °C contains 62,215 kW of cold energy and P1 inputs 402.5 kW of effective energy to increase the LNG pressure to 7500 kPa. Then, 18,185.25 kW of cold energy is consumed in heat exchange with the air, 6187 kW is used by the cold energy generation system, and 402.5 kW is consumed by the air conditioning circulating water. The three-stage compressor inputs 16,094.45 kW of effective energy, while liquid propane (LP) contributes 13,068.4 kW, and the cold box (CB) inputs 16,176.59 kW, including 2215.63 kW from the un-liquefied air return. The J-T process consumes 1811.59 kW, and the heat exchange with the thermal discharge from the power plant requires 580.75 kW. The heat exchangers HX1 to HX4 consume 10,046.84 kW, while the air conditioning circulating water consumes 402.5 kW. The cold energy consumed by heat exchangers HX1 to HX4 totals 10,046.84 kW, with the final output of liquid air having a cold energy value of 48,796.18 kW. The NG cold energy value for 1 °C output from the system is 37,001.25 kW. During the energy release process, LNG continuously gasifies to release cold energy. The high-grade cold energy used to liquefy the air during storage is now recovered by propane, while the remaining LNG cold energy follows the same utilization process as in the storage mode. Liquid air exits the storage tank, is pressurized by P3 with an input of 80.9 kW of effective energy, and then undergoes gasification in the gasification heat exchanger, consuming 21,700.1 kW of cold energy. The heat exchange between the air and the thermal discharge from the power plant consumes 428.73 kW, while heat exchangers HX5 to HX8 account for a loss of 3789.35 kW, and turbines Tur1 to Tur4 consume 4651.32 kW for electricity generation. Finally, the turbine generates a total of 18,490 kW of electricity.

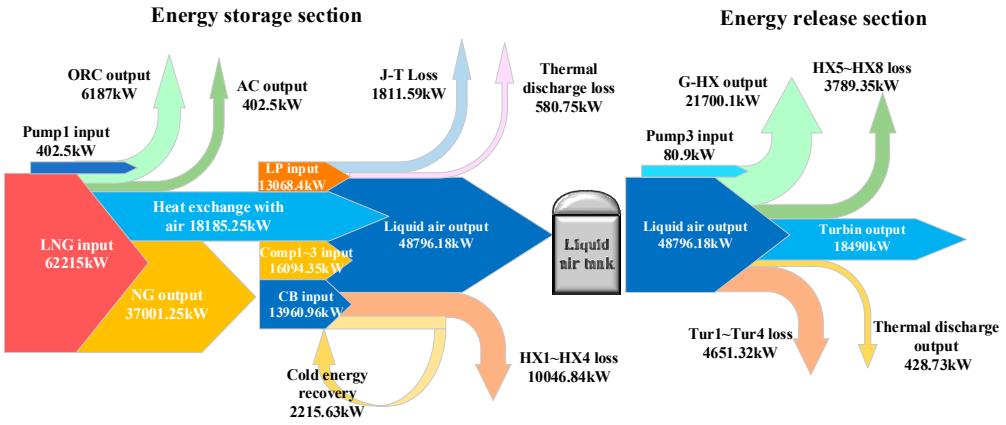


Figure 4. LNG cold energy utilization process exergy flow chart.

4.2.2. Exergy Destruction Analysis

The total system exergy loss is 43,669.24 kW. The exergy loss percentage for each equipment in the system is shown in Figure 5. The largest exergy loss occurs in the heat exchangers (including five multi-strand logistics heat exchangers, the cold box, and the gasification heat exchanger), which account for about 47% of the total loss. This is due to the temperature difference during heat transfer between the LNG and the air or medium, resulting in significant effective energy loss. The next largest loss, about 15%, occurs in the thermal discharge from the power plant heat exchanger, where cold energy released by the low-temperature working mass is carried away by the thermal discharge resulting in effective energy loss. During the energy release process, the heat exchanger in the cold storage unit causes effective energy loss during heat exchange between LNG and propane, accounting for about 13.29%. The three air compressors input a total of 33,271.29 kW of effective energy. However, due to interstage cooling by LNG, the energy consumption and exergy loss of the compressors are reduced, resulting in an exergy loss of only 3465.65 kW, or 8%, with each compressor achieving an exergy efficiency of over 80%. The temperature difference between LNG and the air conditioning circulating water causes an exergy loss of 969.70 kW, or about 2%.

The exergy destruction of the pumps, compressors, and expanders is presented in Table 6. The total input effective energy of the system, including LNG coolant and the energy input to the pumps and compressors, is 47,075.74 kW. The output effective energy consists of the expansion work from the liquid air energy-releasing power generation system, the ORC expansion work, and the electricity used to refrigerate the air conditioning circulating water, totaling 26,310 kW. Thus, the total energy efficiency of the system is 55.89%. This represents an improvement of about 6.18% over the conventional liquid air energy storage system.

Table 6. Exergy destruction and exergy efficiency for pump, turbine and compressor.

Equipment Name		Input Density/kW	Output Density/kW	Exergy Destruction/kW	Exergy Efficiency%
Pump	P1	1178	402.5	775.5	34.17
	P2	46.99	27.78	19.21	59.11
	P3	1077	80.9	996.1	7.5
Compressor	Comp1	7116	5921.13	1194.87	83.21
	Comp2	6628	5453.47	1174.53	82.28
	Comp3	5816	4719.75	1096.25	81.15
Turbin	Tur1	5571.41	4439	1132.41	79.67
	Tur2	5818.02	4647	1171.02	79.87
	Tur3	5957.82	4761	1196.82	79.91
	Tur4	5794.07	4643	1151.07	80.13
	Tur5	2848.40	2820	28.3951	99

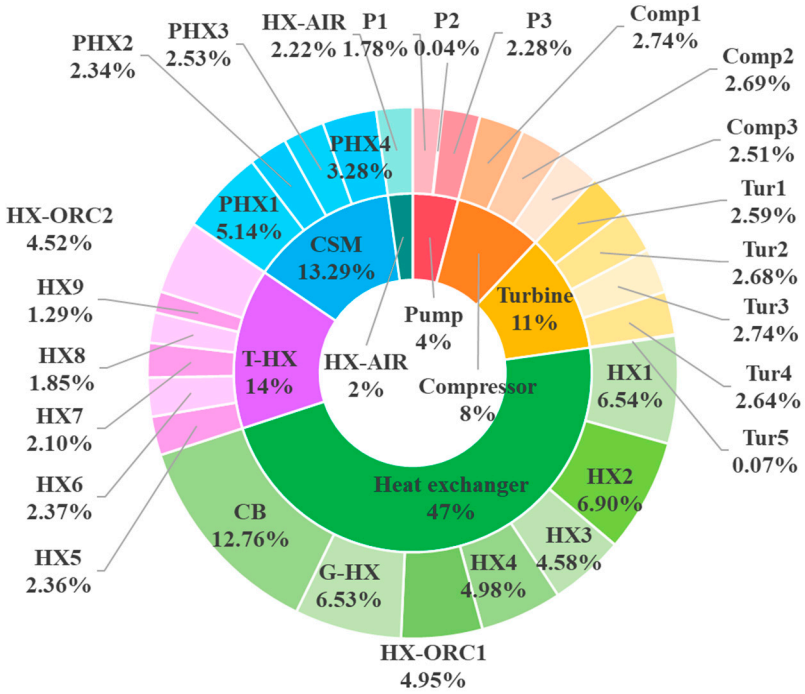


Figure 5. Exergy destruction percentage for each piece of equipment in the system.

4.3. Economic Analysis

Net Present Value (NPV) Analysis

The capital cost includes equipment procurement cost and installation cost. According to the economic analysis module of Aspen HYSYS software V14, the capital costs of each equipment in the system design phase are shown in Table 7, with a total of CNY 156,854,600. According to the electricity price policy for industrial users at an LNG receiving station in Tangshan, Hebei, different electricity prices are applied at different times of the day, with peak electricity price at 0.8473 CNY/kWh and valley electricity price at 0.1233 CNY/kWh.

Table 7. Summary of capital costs for each piece of system equipment.

Equipment Name	Price of Item/Yuan	Quantities/Unit
Tank	12,116,600	5
Compressor	11,489,400	3
Turbin	2,091,200	5
Heat exchangers	2,412,900	18
Pump	2,638,400	3

Due to the use of propane tanks as intermediate storage, the system has flexible energy storage and release capabilities, which can flexibly generate electricity according to users' electricity demands. The cold energy power generation system operates along with the vaporization of LNG. During the energy storage period, the ORC system can provide partial electrical energy for the three compressors. During the energy release period, the ORC system and the liquid air energy release system generate electricity together. The cooling capacity provided by the cold energy air conditioning can save 5000 kW of electrical energy, which can also be considered as part of the project's revenue.

The plant's service life is calculated as 25 years, with a discount rate of 7%, a tax rate of 25%, a daily working time of the system of 22 h, a daily peak electricity time of 11 h, and a daily off-peak electricity time of 11 h. The air conditioning working time is calculated as 90 days per year, with 22 h of work each day.

As shown in Figure 6, when conducting an economic analysis of this project using the net present value method, the net present value is calculated to be CNY 566,413,500, and the project can recover its initial investment cost within 2.53 years. The annual operating cost of the project is CNY 149,952,000, of which the electricity consumption cost is CNY 102,896,000 and the maintenance cost is CNY 47,056,000. The total revenue of the project is CNY 770,592,000, which includes two parts: one is the CNY 686,710,000 obtained from selling electricity during peak electricity periods, and the other is the CNY 83,883,000 saved from air conditioning electricity costs.

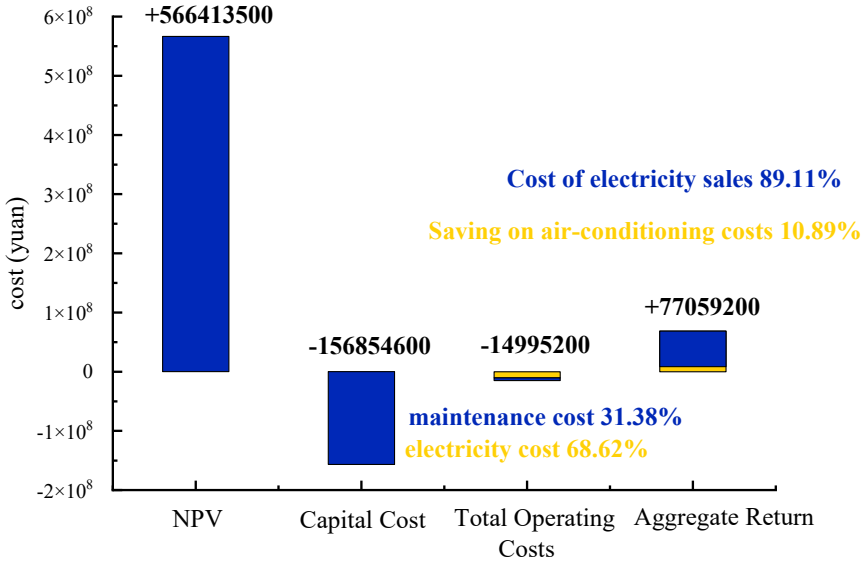


Figure 6. Results of net present value analysis.

5. Conclusions

This research presents a new LAES system, aiming to tackle the issues of low efficiency and limited practical value in existing LAES systems, and the inability of LNG cold energy power generation to balance power supply and demand. The system stores the cold energy released during LNG gasification in low-price electricity periods and releases it during high-price periods, also cascading the use of LNG cold energy to boost system performance.

(1) By replacing the electricity-driven cryogenic cooling process with LNG cold energy, the system attains a cycling efficiency of 105.83%, versus the 50% to 70% efficiency of traditional LAES systems.

(2) Simulations show that the system has an overall exergy efficiency of 55.89%, a 6.18% increase from conventional LAES systems. The cascading design uses the LNG's cryogenic zone (−162 °C to −80 °C) for LAES, its mid-temperature zone (−80 °C to −45 °C) to drive an ORC power generation system, and its high-temperature zone (−45 °C to 1 °C) for air conditioning cooling. This design effectively reduces exergy losses due to temperature differences in heat transfer. Although heat exchanger groups have the largest proportion of exergy losses at 47%, the compression group's exergy efficiency stays above 80%.

(3) Based on the peak–valley electricity prices in the Tangshan area, the system generates an annual revenue of CNY 77.06 million, with a net present value (NPV) of CNY 566.41 million and a capital payback period of just 2.53 years. During the energy-release phase, power generation revenues are CNY 68.67 million per year, and energy-saving revenues from cold energy air conditioning reach CNY 8.39 million per year. Annual operating costs are CNY 14.99 million (including CNY 4.71 million

for maintenance). The economic model confirms the system's commercialization potential in areas with high peak-shaving demand.

(4) The system uses the thermal discharge from the power plant during the LNG gasification process. This not only cuts down the cooling steps for the power plant but also offers a heat source for LNG cold energy recovery, avoiding ocean thermal pollution. This improves both economic and environmental performance.

Author Contributions: Conceptualization, Z.L. and X.S.; methodology, Z.L. and H.Z.; software, Z.L. and Y.Z.; validation, X.S.; formal analysis, Y.Z.; investigation, Y.Z.; resources, H.Z.; data curation, H.Z.; writing—original draft preparation, Z.L.; writing—review and editing, Z.L. and Y.G.; visualization, Z.C.; supervision, Z.C.; project administration, Y.G.; funding acquisition, Y.G. All authors have read and agreed to the published version of the manuscript.

Funding: This work was funded by S&T Program of Hebei, grant number 242Q4502Z.

Data Availability Statement: The authors confirm that the data supporting the findings of this study are available within the article.

Conflicts of Interest: Authors Xiaolei Si, Hongyan Zhao and Zheng Cai were employed by the company Caofeidian Xintian LNG Co., Ltd. Author Yongchao Zhao was employed by the company Suntien Green Energy Co., Ltd. The remaining authors declare that the research was conducted in the absence of any commercial or financial relationships that could be construed as a potential conflict of interest.

Abbreviations

The following abbreviations are used in this manuscript:

LNG	Liquefied Natural Gas
NG	Natural Gas
LAES	Liquid Air Energy Storage
ORC	Organic Rankine Cycle
PTST	Propane Thermal Storage Tank
PCST	Propane Cryogenic Storage Tank
HST	Heat Storage Tank
CST	Cryogenic Storage Tank
LP	Liquid Propane
CB	Cold Box
HX	Heat Exchanger
P	Pump
Comp	Compressor
Tur	Turbin
G-HX	Gasification heat exchanger

References

1. Li, B.; Xie, H.; Sun, L.; Gao, T.; Xia, E.; Liu, B. Advanced exergy analysis and multi-objective optimization of dual-loop ORC utilizing LNG cold energy and geothermal energy. *Renew. Energy* **2025**, *239*, 122164. [CrossRef]
2. Qi, Y.; Zuo, P.; Lu, R.; Wang, D.; Guo, Y. Modeling of Liquefied Natural Gas Cold Power Generation for Access to the Distribution Grid. *Energies* **2024**, *17*, 5323. [CrossRef]
3. Cao, S.; Luan, T.; Zuo, P.; Si, X.; Xie, P.; Guo, Y. Simulation and Economic Benefit Analysis of Carburetor Combined Transport in Winter at a Liquefied Natural Gas Receiving Station. *Energies* **2025**, *18*, 276. [CrossRef]
4. He, T.; Chong, R.Z.; Zheng, J.; Ju, Y.; Linga, P. LNG cold energy utilization: Prospects and challenges. *Energy* **2019**, *170*, 557–568. [CrossRef]
5. Zheng, X.; Zhang, J.; Li, Y.; Zhang, Z. Performance analysis and multi-objective optimization for an integrated air separation, power generation, refrigeration and ice thermal storage system based on the LNG cold energy utilization. *Int. J. Refrig.* **2024**, *130*, 521–536. [CrossRef]

6. Jia, H.; Zhang, G.Z.; Dong, W.Q.; Sun, L.; Zhang, P. Comparative study on cold energy utilization schemes of liquefied natural gas. *Petrochem. Ind. Technol.* **2023**, *30*, 13–15.
7. Wang, F.; Li, P.; Gai, L.; Chen, Y.; Zhu, B.; Chen, X.; Tao, H.; Varbanov, P.S. Enhancing the efficiency of power generation through the utilisation of LNG cold energy by a dual-fluid condensation rankine cycle system. *Energy* **2024**, *305*, 132113. [CrossRef]
8. Cai, D.; Zhao, Y.; Wang, Y.; Liu, H.; Liang, Y.; Hu, D. Comparative analysis: Exergetic and economic assessment of LNG cold energy power generation systems with different cold utilization methods. *Therm. Sci. Eng. Prog.* **2024**, *54*, 102844. [CrossRef]
9. Liang, T.; Li, Y.; Nie, B.; Ahmad, A.; Ding, Y. Achieving a net-zero-carbon energy system in the UK by 2050 with liquid air energy storage. *Energy Convers. Manag.* **2025**, *327*, 119524. [CrossRef]
10. Yang, M.; Tong, Y.; Wang, J.; Duan, L.; Zhang, H.; Yang, C.; Wang, Q.; Ding, X. Design optimization and techno-economic performance comparisons of different solar aided liquid air energy storage systems. *Therm. Sci. Eng. Prog.* **2025**, *59*, 103267. [CrossRef]
11. Lis, P.; Milewski, J.; Ryś, P.; Shuhayeu, P. A fluid flow machine unit for a small-scale compressed gas energy storage system–Literature review. *Appl. Energy* **2025**, *383*, 125312. [CrossRef]
12. Shi, X.; He, Q.; Wang, K.; Chen, H.; Du, D. Energy, exergy and economic analysis of a novel multi-generation liquefied air energy storage system coupled with coal-fired power unit based on ejector and absorption refrigeration. *Energy Convers. Manag.* **2025**, *326*, 119540. [CrossRef]
13. Wang, X.; Wang, C.; Xu, Y.; Zhang, Z.; Han, P.; Li, Y.; She, X. Thermodynamic analysis of a novel multi-layer packed bed cold energy storage with low exergy loss for liquid air energy storage system. *Renew. Energy* **2025**, *240*, 122271. [CrossRef]
14. Fan, M.; Liu, C.; Tong, L.; Yin, S.; Zhang, P.; Zuo, Z.; Wang, L.; Ding, Y. A cold thermal energy storage based on ASU-LAES system: Energy, exergy, and economic analysis. *Energy* **2025**, *314*, 134132. [CrossRef]
15. Pan, C.; Jiang, Q.; Feng, G.; Feng, H.; Lu, X.; Meng, B.; Gu, J.; Jiang, Z. Thermodynamic analysis of liquefied air energy storage system by using LNG cold energy. *Cryog./Refrig.* **2022**, *50*, 57–63.
16. Qi, M.; Park, J.; Kim, J.; Lee, I.; Moon, I. Advanced integration of LNG regasification power plant with liquid air energy storage: Enhancements in flexibility, safety, and power generation. *Appl. Energy* **2020**, *296*, 115049–115066. [CrossRef]
17. Li, J.; Fan, X.; Li, Y.; Wang, Z.; Gao, Z.; Ji, W.; Chen, L.; Wang, J. A novel system of liquid air energy storage with LNG cold energy and industrial waste heat: Thermodynamic and economic analysis. *J. Energy Storage* **2024**, *86*, 111359. [CrossRef]
18. Kim, Y.; Mun, H.; Kim, M.; Moon, I.; Park, J.; Lee, I.; Kim, J. Design and global sensitivity analysis of a flexible hydrogen regasification process integrated with liquid air energy storage system. *Energy* **2025**, *316*, 134533. [CrossRef]
19. Duan, Z.; Wang, K.; Cao, Y.; Wang, J.; Liu, Q. Multi-objective optimization of thermodynamics parameters of a biomass and liquefied natural gas complementary system integrated with liquid air energy storage and two-stage organic Rankine cycles. *Energy* **2025**, *314*, 134171. [CrossRef]
20. Liu, H.; Tang, L.; Dou, Z.; Wang, S.; Yu, D. Optimizing integrated hydrogen liquefaction with LNG cold energy: A thermoeconomic assessment, comparative analysis, and feasibility study with emphasis on composite curves and uncertainty scrutiny. *Energy* **2025**, *315*, 134416. [CrossRef]
21. Tauseef, M.N.; Mirae, K.; Jaehwa, L.; Kim, S.; Kim, K.C. A review on technologies with electricity generation potentials using liquified natural gas regasification cold energy. *Front. Energy* **2023**, *17*, 332–379.
22. Si, H.; Chen, S.; Xie, R.; Zeng, W.Q.; Zhang, X.J.; Jiang, L. Techno-economic analysis on a hybrid system with carbon capture and energy storage for liquefied natural gas cold energy utilization. *Energy* **2024**, *308*, 132958. [CrossRef]
23. Zhang, C.; Li, D.; Mao, C.; Liu, H.; Chen, Y. Thermodynamic analysis of liquid air energy storage system integrating LNG cold energy. *Energy* **2024**, *299*, 131485. [CrossRef]
24. Wang, Z.; Li, J.; Li, Y.; Fan, X.; Gao, Z.; Ji, W.; Chen, L.; Wang, J. Thermodynamic and economic analysis of multi-generation system based on LNG-LAES integrating with air separation unit. *Energy* **2024**, *306*, 132441. [CrossRef]
25. Qi, Y.; Zuo, P.; Wang, D.; Cai, Z.; Guo, Y. Multi-Port Converter Design Solution for LNG Cold Power Generation. In Proceedings of the 2024 Asia Power and Electrical Technology Conference (APET), Fuzhou, China, 15–17 November 2024; pp. 632–635.
26. Li, J.; Liu, Y.; Liu, K.; Gao, S. Chen, L. Wang, J. Optimization and performance evaluation for liquid air energy storage based on liquid natural gas cold energy utilization. *Therm. Power Gener.* **2024**, *53*, 69–77.
27. Su, Y.; Wu, X.; Liao, B.; Li, S. Analysis of novel liquefied-air energy-storage system coupled with LNG cold energy and ORC. *Energy Storage Sci. Technol.* **2022**, *11*, 1996–2006.

Disclaimer/Publisher's Note: The statements, opinions and data contained in all publications are solely those of the individual author(s) and contributor(s) and not of MDPI and/or the editor(s). MDPI and/or the editor(s) disclaim responsibility for any injury to people or property resulting from any ideas, methods, instructions or products referred to in the content.